

# Magnetic Properties of Ultrafine $\epsilon$ -Fe<sub>2</sub>O<sub>3</sub> Nanoparticles in a Silicon Xerogel Matrix

Yu. V. Knyazev<sup>a,\*</sup>, S. S. Yakushkin<sup>b</sup>, D. A. Balaev<sup>a</sup>, A. A. Dubrovsky<sup>a</sup>, S. V. Semenov<sup>a</sup>,  
O. A. Bayukov<sup>a</sup>, V. L. Kirillov<sup>b</sup>, and O. N. Martyanov<sup>b</sup>

<sup>a</sup>Kirensky Institute of Physics, Krasnoyarsk Scientific Center, Siberian Branch, Russian Academy of Sciences, Krasnoyarsk, 660036 Russia

<sup>b</sup>Boreskov Institute of Catalysis, Siberian Branch, Russian Academy of Sciences, Novosibirsk, 630090 Russia  
\*e-mail: yuk@iph.krasn.ru

Received September 7, 2018; revised January 31, 2019; accepted March 27, 2019

**Abstract**—A new metamaterial is obtained on the basis of  $\epsilon$ -Fe<sub>2</sub>O<sub>3</sub> nanoparticles immobilized in a xerogel matrix. Samples are synthesized by impregnating SiO<sub>2</sub> hydrogel with iron (II) salts with subsequent drying and calcination. The structure and magnetic properties of the composites are probed using transmission electron microscopy, X-ray diffraction, Mössbauer spectroscopy, and static magnetic measurements.

DOI: 10.3103/S1062873819070219

## INTRODUCTION

$\epsilon$ -Fe<sub>2</sub>O<sub>3</sub> is known to be a unique form of iron oxide, due to its elevated coercivity [1–3] and high frequency absorption in the millimeter wave range [1, 4–6]. This phase exists in only nanoparticle form in the presence of SiO<sub>2</sub> [7, 8]. The difficulty in producing  $\epsilon$ -Fe<sub>2</sub>O<sub>3</sub> nanoparticles without other kinds of iron oxides results in the need to control particle size, and to prevent agglomeration. The crystal structure of this polymorph contains four nonequivalent iron positions, three of which have an octahedral environment while one has tetrahedral ambience. According to different sources, the magnetic ordering temperature for  $\epsilon$ -Fe<sub>2</sub>O<sub>3</sub> varies from 500 to 850 K [1, 9]. In addition, there is one more magnetic transition in the temperature range of 80–150 K that is associated with the re-orientation of magnetic moments from predominately tetrahedral iron positions. This transition was detected from the magnetic, neutron diffraction, and Mössbauer spectroscopy data in [1, 4] for nanoparticles with sizes of 10–40 nm.

## EXPERIMENTAL

In this work,  $\epsilon$ -Fe<sub>2</sub>O<sub>3</sub> particles in xerogel ( $\epsilon$ -Fe<sub>2</sub>O<sub>3</sub> content, 20 wt %) were synthesized by embedding iron (II) salt (FeSO<sub>4</sub> · 7H<sub>2</sub>O) in a SiO<sub>2</sub> xerogel via diffusion exchange in a H<sub>2</sub>SO<sub>4</sub> aqueous solution (pH 2). At the next stage, the gel was dried in air for several days and then exposed to air drying at 110°C for 4 h. It was finally annealed at 900°C with subsequent cooling to room temperature. This enabled us to obtain samples

with  $\epsilon$ -Fe<sub>2</sub>O<sub>3</sub> nanoparticles immobilized in a xerogel (SiO<sub>2</sub>) matrix.

Transmission electron microscopy (TEM) measurements were made using a JEOL JEM-2010 microscope with an accelerating voltage of 200 kV and a resolution of 1.4 Å. Our X-ray diffraction study was performed on an XTRA (Switzerland) powder diffractometer and a D8 Advance Bruker (Germany) unit using CuK $\alpha$  radiation at a wavelength  $\lambda = 1.5418$  Å. Our Mössbauer spectroscopy experiments were conducted in the temperature range of 4–300 K, using a MC-1104EM spectrometer with a Co<sup>57</sup>(Rh) source and a helium cryogenic refrigeration system (OOO Kriotreid). The magnetic properties were examined with a vibration magnetometer (sensitivity, 10<sup>-5</sup> emu). The data were normalized to the weight of  $\epsilon$ -Fe<sub>2</sub>O<sub>3</sub> in the samples.

## RESULTS AND DISCUSSION

A TEM optical micrograph of nanoparticles in a xerogel matrix is shown in Fig. 1a. According to our TEM and XRD data, the interplane distance corresponded to the lattice parameters of  $\epsilon$ -Fe<sub>2</sub>O<sub>3</sub>. The average particle size in each sample was 8 nm. As was shown in our earlier work, spatial stabilization of nanoparticles during calcination is a key factor in obtaining an  $\epsilon$ -Fe<sub>2</sub>O<sub>3</sub> phase free from impurities of other iron oxide modifications [10].

Figure 1b presents the room temperature Mössbauer spectra of samples. The spectra were processed by means of linear least squares. All four of the non-

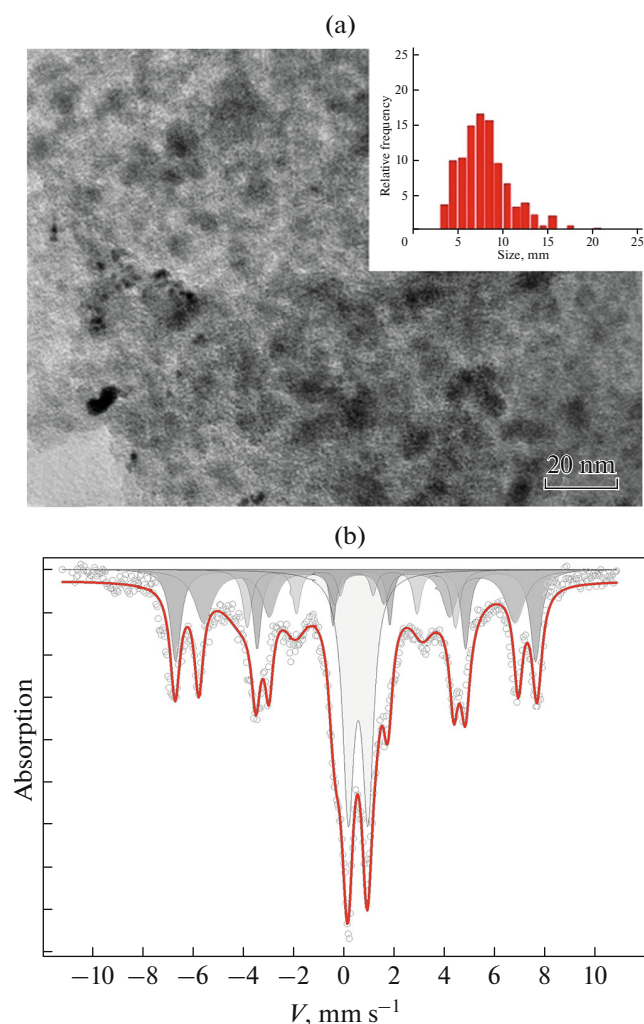


**Fig. 1.** (a) Electron microscope image and (b) Mössbauer spectrum at 300 K. The superparamagnetic part of the spectrum is indicated by the doublet (shading).

equivalent crystallographic iron positions typical of  $\epsilon$ - $\text{Fe}_2\text{O}_3$  were resolved. The iron cations were found to be in a high-spin trivalent state. The spectrum at 300 K revealed a superpositioning of magnetic and paramagnetic components in the form of Zeeman sextets and the quadrupole doublet, respectively. The paramagnetic component in the spectra was due to the presence of nanoparticles in the unlocked (superparamagnetic) state. The lower the temperature, the higher the number of locked nanoparticles, enlarging the area beneath the magnetic part in the spectrum.

According to our magnetic measurements [11], the locking temperature was 30 K. The room temperature coercive force was 3.7 kOe (Fig. 2). A drop in temperature causes a nonmonotonic change in the hysteresis loop width. The waists of the loops observed in the range of the magnetic transition (80–150 K), were due to the paramagnetic contribution from small nanoparticles, for which the locking temperature was 30 K [11].

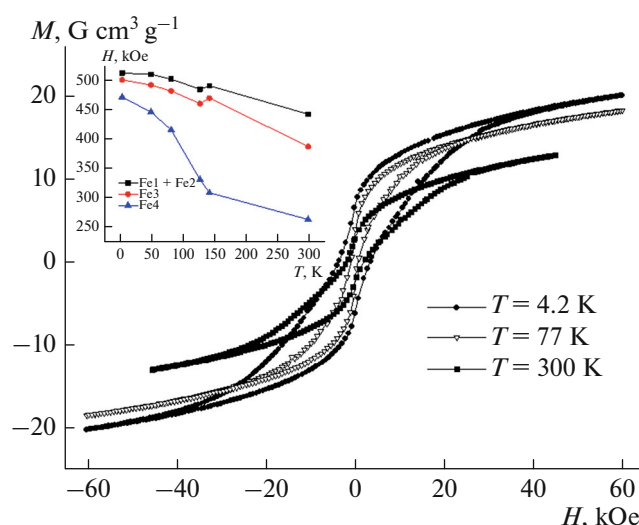


**Fig. 2.** Field dependences of the magnetization of  $\epsilon$ - $\text{Fe}_2\text{O}_3$  nanoparticles in a xerogel matrix. The insert shows the temperature dependence of the ultrathin field, obtained via Mössbauer spectroscopy.

Since the concentration of nanoparticle weight in the xerogel matrix was relatively low, the interactions between the particles can be ignored, so the locking temperature was determined by the properties of each individual nanoparticle (or its energy of magnetic anisotropy). The locking temperature thus depends on the size of a specific nanoparticle only, while the non-magnetic matrix has no visual effect on this parameter.

The Mössbauer spectra recorded when there was no magnetic field reveal variation in the ultrathin field of the iron cations in the range of the magnetic transition at temperatures of 4–300 K. The insert in Fig. 2 presents the ultrathin fields as a function of temperature for each nonequivalent position in  $\epsilon$ - $\text{Fe}_2\text{O}_3$ . The increase in the ultrathin field of the iron nuclei with a tetrahedral environment (Fe4) is approximately 30%, which testifies to the existence of the magnetic transition and coincides for larger particles [1]. It is also worth noting that the nature of this transition remains a topic of debate [1, 4].

## CONCLUSIONS

An original approach to synthesizing  $\epsilon$ - $\text{Fe}_2\text{O}_3$  nanoparticles in a xerogel matrix was proposed. Study of the structure via transmission electron microscopy and X-ray diffraction confirmed the absence of any other polymorphous iron oxides as impurities. Mössbauer microscopy confirmed the existence of four iron cations, localized at the octahedral and tetrahedral positions typical of the  $\epsilon$ - $\text{Fe}_2\text{O}_3$  phase. Magnetic properties were analyzed through low temperature Mössbauer spectroscopy and measurements of the associated force. The change in the ultrathin magnetic

field detected via Mössbauer spectroscopy in a sample with an average particle size of 8 nm revealed the magnetic transition occurs in the temperature range of 80–150 K at any particle size.

## REFERENCES

1. Gich, M., Frontera, C., Roig, A., et al., *Chem. Mater.*, 2006, vol. 18, p. 3889.
2. Dubrovskiy, A.A., Balaev, D.A., Shaykhutdinov, K.A., et al., *J. Appl. Phys.*, 2015, vol. 118, p. 213901.
3. Jin, J., Ohkoshi, S., and Hashimoto, K., *Adv. Mater.*, 2004, vol. 16, p. 48.
4. Tuček, J., Zbořil, R., Namai, A., et al., *Chem. Mater.*, 2010, vol. 22, p. 6483.
5. Tronc, E., Chanéac, C., and Jolivet, J.P., *J. Solid State Chem.*, 1998, vol. 139, p. 93.
6. Ohkoshi, S., Kuroki, S., Sakurai, S., et al., *Angew. Chem. Int. Ed.*, 2007, vol. 46, p. 8392.
7. Ohkoshi, S., Sakurai, S., Jin, J., et al., *J. Appl. Phys.*, 2005, vol. 97, p. 10K312.
8. Sakurai, S., Namai, A., Hashimoto, K., et al., *J. Am. Chem. Soc.*, 2009, vol. 131, p. 18299.
9. García-Muñoz, J.L., Romaguera, A., Fauth, F., et al., *Chem. Mater.*, 2017, vol. 29, no. 22, p. 9705.
10. Yakushkin, S.S., Bukhtiyarova, G.A., and Martyanov, O.N., *J. Struct. Chem.*, 2013, vol. 54, p. 876.
11. Yakushkin, S.S., Balaev, D.A., Dubrovskiy, A.A., et al., *Ceram. Int.*, 2018, vol. 44, p. 17852.

*Translated by O. Maslova*